

Line-Circle: A Geometric Filter for Single Camera Edge-Based Object Detection

Seyed Amir Tafirishi

Department of Automation and
Control Systems, University of Sheffield,
Sheffield, UK
Email: amirtafirishi@yahoo.com

Vahid E. Kandjani

Department of Information
Technology, University College of
Nabi Akram, Tabriz, IRAN
Email: esmaeilzadeh_v@kish.sharif.edu

Abstract—This paper presents a state-of-the-art approach in object detection for being applied in future SLAM problems. Although, many SLAM methods are proposed to create suitable autonomy for mobile robots namely ground vehicles, they still face overconfidence and large computations during entrance to immense spaces with many landmarks. In particular, they suffer from impractical applications via sole reliance on the limited sensors like camera. Proposed method claims that unmanned ground vehicles without having huge amount of database for object definition and highly advance prediction parameters can deal with incoming objects during straight motion of camera in real-time. Line-Circle (LC) filter tries to apply detection, tracking and learning to each defined experts to obtain more information for judging scene without over-calculation. In this filter, circle expert let us summarize edges in groups. The Interactive feedback learning between each expert creates minimal error that fights against overwhelming landmark signs in crowded scenes without mapping. Our experts basically are dependent on trust factors' covariance with geometric definitions to ignore, emerge and compare detected landmarks. The experiment for validating the model is taken place utilizing a camera beside an IMU sensor for location estimation.

NOMENCLATURE

λ	Collector for grouping landmarks.
ψ	The ignorance parameter.
E_n, E_r	Normal and rebel edges matrices.
C_n, C_r	Normal and rebel collected landmark matrices in Circle expert.
α	Scaling parameter to determine rebel edges.
L	Edge location on the captured frame.
BS, BL	Boundary size of λ and E_n .
DL	Deviation level of rebel edges.
R	Radius of given scaling/temporary parameters.
T_y	Type of found ignorance region
Tr	Trust factor.
β_q	Relevant angle of edge or experts.
V_q	Velocity magnitude of edge or experts.
O	Existing origin point for rebel landmarks.
δ	Governing error matrix.
$Edge$	Current frame's edges.

I. INTRODUCTION

In the most of autonomous driving systems, it is important to detect objects along the direction of moving vehicle. Mobile robots have limited source of power and require fast responses

during their motion. Additionally, it is an urge to reduce resources and sensors during active times [1]. There have been some studies on object detection and mapping to enhance the performance and decrease the computation [1]- [14]. These detectors are using real-time data to process during their activation states.

Different detection methods have been studied to create accurate and fast analysis over the surrounding. Eade and Drummond proposed a machine learning corner detection method to be used as the first monocular SLAM systems capable of operating in real-time [3]. As a classic approach for understanding the environment the stereo-based model was firstly designed by Murray and Little for SLAM operations [4]. Other detection methods were studied related to the point analysis [5] and image contouring [6]. Recently, semi-dense monocular SLAM with integration of color was applied to determine the surrounding objects at MIT [7]. Lastly, an overall review was presented by Sun et al about localizing other vehicles on the road [8].

Monocular SLAM with corner detection as the most practical and advance method, was analyzed to have better solutions for overconfidence and dealing with high computations related to detected landmark. Lui and Drummond proposed a new system for constant time monocular SLAM that uses only 2D measurement and takes the image graph with sparse pairwise geometric. There were some improvements such as no global consistency and bundle adjustments but the system was based on multi-camera perspective and it was also dependent on a reference image [9]. As a alternative, Kalman filter reduction was operated for SLAM problems for using bundle adjustment by sparse matrix and double windowing method [10]. Gamage and Drummond tried to decrease dimension of the covariance matrices of camera and landmark position. Although it minimized some nonlinearities that creates inconsistency in EKF, it was not able to deal with overwhelming landmarks. A requirement for solely image-based filter as a superior method rather than a classic Kalman filter has been remained unsatisfactory. Vision dependent applications require filter that is able to do real-time computation reduction within diverse machine learning evaluation layers.

In this paper we constructed a filter for solely 2D image utilization about object detection. In following work, via using

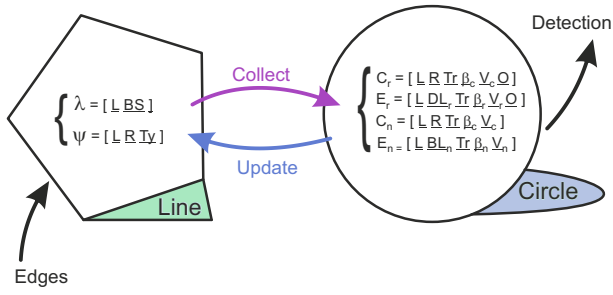


Fig. 1. The map of geometric filter.

a real-time captured data parallel to the internal measurement unit (IMU), a scene is utilized to predict possible objects that are passing or moving towards our vehicle. Additionally, by using velocity and vehicle dynamics, this filter optimizes the data collection from existing edge detection methods or event-base camera [11] to ignore/concentrate on particular landmarks. Beside these capabilities, with certain inspiration from estimators namely Kalman Filter, errors are minimized to prevent any wrong or integrated uncertainties of detected landmarks.

II. LINE-CIRCLE (LC) FILTER

The filter is proposed in a way that the mainframe system have its evaluation from surroundings in real-time. The algorithm basically understands and creates the object locations with its past information and currently obtained data from camera and IMU sensors. The novelty of approach stands about its multi-level analysis on captured edge from corner detection method [3], [12]. Fundamentally, this method carries its environmental analysis with filtering the data in each state of experts (line and circle) to update the previous one for future incoming frames beside next expert. The overall frame studies have been mapped like an interactive transitional-base principles with main parameter flow for detection, learning and tracking the incoming detected corners [see Fig. 1].

Scaling and temporary parameters are two groups in this approach. In former, λ is responsible for grouping the edges with L location and BS boundary size. ψ is a feedback parameter for λ in which it takes the information from circle to create ignorance regions via L , R and Ty as the location, radius of ignorant and a flag for ignoring geometry type. ψ avoids trusted overloading edges involvement in flow of analysis so it helps the robot to process faster and concentrate more on the essential locations. Parameters in latter are temporary information carriers from previous frames. E_n and E_r are the parameters responsible for estimated edges to determine their properties. Beside these parameters in Circle Expert, C_n and C_r will assist the system to collect edges with relevant properties to prepare it for understanding objects without requirement to know their formations. Each parameter has a collection series of information about L location, R/BL_q size of space, Tr trust factor beside β_q , V_q as the angle and velocity of

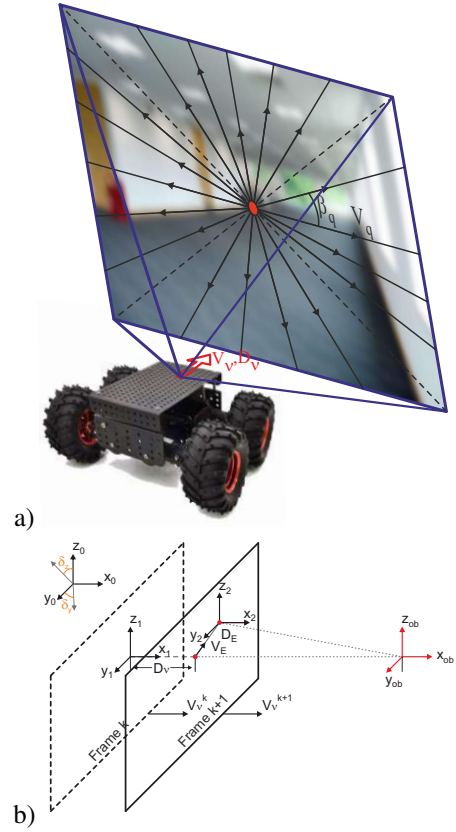


Fig. 2. Kinematic analysis of locomotion with orientated vector field in frame. a) The general view b) Kinematic analysis of edges motion respect to frame and corresponding object.

corresponding motion parameters. O stands for the originated landmark for rebel parameters.

We have four transitions in this machine learning algorithm. Each transition carries detection, learning and tracking applications working with feeding data to experts. Therefore, It explains our dynamic modeled approach that works in integration without sole reliance on a pyramidal supervisory [13]. In first step (base transition), the camera collects the detected edges and groups/omits them with relative feedbacks from previous steps in Line Expert. Next, collection transition happens to categorize the edge groups with reliance on their behaviors to create circles with taken feedback. As a final stage, the estimated variables are presented to have classified data from truly existing objects in Circle expert. The basic kinematic analysis beside parameter definition are as Fig. 2 where mobile robot follows a straight line.

As an important fact, the flow distribution and intensity of vector field is related to plain angle, robots rotation and locomotion velocity. In this practice [see Fig. 2 case b], the two frame information is used where the collected information about vehicles D_v and V_v are compared mathematically for deriving the relevant D_e and V_e of relevant edge. Because in this work, it is assumed that camera just moves in straight line, any angular motion in z and y axes are feed as error $\delta_{z,y}$.

As a simple explanation, Line obtains the edges and classi-

- λ_2^* : By being in BL area and satisfying the error span this will be normal edge which is the suitable candidate for evaluation. Also, the trust of corresponding edge will be upgraded as +1.

- λ_3^* : This edge despite the satisfaction in BL region was failed from V_e and B_e characteristics. Furthermore, It will be required to upgraded with error inclusion. Nevertheless, the trust value for estimated edge will be upgraded as -1.

- λ_4^* : With breaking all the laws depending on the V_e , β_e , BL and error span, it will be considered as rebel edge or new normal landmark depending on the incoming frame rebel edge evaluations. The trust value of estimated edge will remain the same. A new normal edge with average standard and critical trusts will be constructed.

- λ_5^* : Despite exclusion from estimated edge BL , it is in the flow line of error span within BL of previous edge itself. It is assumed as rebellious landmark which leads rebel edge category for further evaluations. The trust of normal edge will be decreased and it will be estimated as $E_n'(k)$ but data will be carried to α for validation of possible E_r existence.

In initialization of E_n , landmarks are placed with no estimation which edge carries its velocity as the vehicle velocity and angle is defined depending on the frame center O beside initial BS_0 . Later on, the normal edges E_n are detected from (1) and error span as:

$$\frac{|-(Edge_x - IC_x) + m_e(Edge_y - IC_y)|}{(1 + m_e^2)^{\frac{1}{2}}} < \delta_{y-z}^v \quad (3)$$

Where $IC_{x,y}$ and m_e are the image center locations and slope of $N_{th} E_n$ respect to frame center. E_n is estimated with beneath formulas for edges location, velocity and boundary layer:

$$\begin{aligned} L_{E_n}(k) &= \frac{(Tr_{E_n}(k-1) - Tr_{cr})L'_{E_n}(k-1) + L_{Edge}(k)}{(Tr_{E_n}(k-1) - Tr_{cr}) + 1} \\ V_{E_n}(k) &= |V_v(k) \\ &\pm \frac{(L'_{E_{nx}}(k-1) - Edge_x)^2 + (L'_{E_{ny}}(k-1) - Edge_y)^2}{t_f}| \quad (4) \\ BL_{E_n}(k) &= \frac{1}{2} \left[\frac{|V_v(k) - V'_{E_n}(k-1)|}{Corr(Edge_{group}^n)} + BL_{E_n}(k-1) \right] \end{aligned}$$

Because it is assumed model is able to recover the error δ_{y-z}^v , β_{E_n} is remained unchanged in straight camera motion. Also, as β_{E_n} has to be estimated in the first step to determine corresponding edge, the error velocity is using $V'_{E_n}(k-1) = \frac{1}{2}[V_{E_n}(k-1) + V_v]$. t_f is the spending time from previous frame till the current Circle expert run.

For determining the rebel edges E_r detections, we proposed line tracking model that tries to eliminate these edges with N frame steps [see Fig. 4]. By presenting the minimum $N = 3$ frame per sec, we sum the detected landmarks by following their left marks from previous steps. We apply the model with considering underneath specifications:

- Due to unexpected motion in the rebellious landmarks for consecutive frames, tracking will be a non-linear motion with a certain deviation in each frame.

Algorithm 2 Circle Expert, Edge Estimation Part

```

1: procedure CIRCLE( $Edge, C_n, C_r, E_n, E_r, \Psi, \delta, V_v, D_v$ )
2:   if  $E_n = \emptyset$  then                                      $\triangleright$  Edge matching
3:     Initialize  $E_n$  with  $Edge$ 
4:   else
5:     while All the edges in  $E_n$  are checked do
6:       while All the  $Edge$  groups are checked do
7:         Find matching landmark group of  $Edges$ 
8:         if  $N^{th} E_n'$  satisfies  $\lambda_{2,3}^*$  then
9:           Find nearest  $Edge$  in boundary
10:          Update  $N^{th} E_n$ 
11:          Remove landmark from  $Edge$ 
12:         else if  $N^{th} E_n'$  satisfies  $\lambda_5^*$  then
13:           Update  $N^{th} E_n$ 
14:           Apply rebel detection with  $\alpha$ 
15:           Remove landmark from  $Edge$ 
16:         else if No  $E_n'$  match then
17:            $N^{th} E_n \leftarrow N^{th} E_n'$ 
18:           Update  $N^{th} E_n$  remaining param.
19:         end if
20:       end while
21:     end while
22:   if  $E_r = \emptyset$  then
23:     else
24:       while All the edges  $E_r$  are checked do
25:         while All the  $Edge$  are checked do
26:           Find landmark from  $Edges$ 
27:           if  $N^{th} E_r'$  satisfies  $\lambda_r^*$  then
28:             Update  $N^{th} E_r$ 
29:             Remove landmark from  $Edge$ 
30:           else if No  $E_r'$  match then
31:              $N^{th} E_r \leftarrow N^{th} E_r'$ 
32:             Update  $N^{th} E_n$  remaining param.
33:           end if
34:         end while
35:       end while
36:     end if
37:   end if
38:   Add left  $Edge$  as new  $E_n$  ( $\lambda_{1,4}^*$ )    $\triangleright$  Edge matching
39:   return  $E_n, E_r, \alpha$ 

```

- The number of frame to evaluate the reliability of existing detection to rebel landmarks will be 3.

- The relation of the connected landmarks are deleted after success/fail in three frame analysis of α .

The α scaling parameter basically works as following:

$$\alpha \propto \left\{ \sum_{L_n, \ell}^3 \right\} \quad (5)$$

Where L_n is the located edges positions on frame and ℓ is the number of frames that the involved edges are checked. However, this study includes the error span as well in this for-

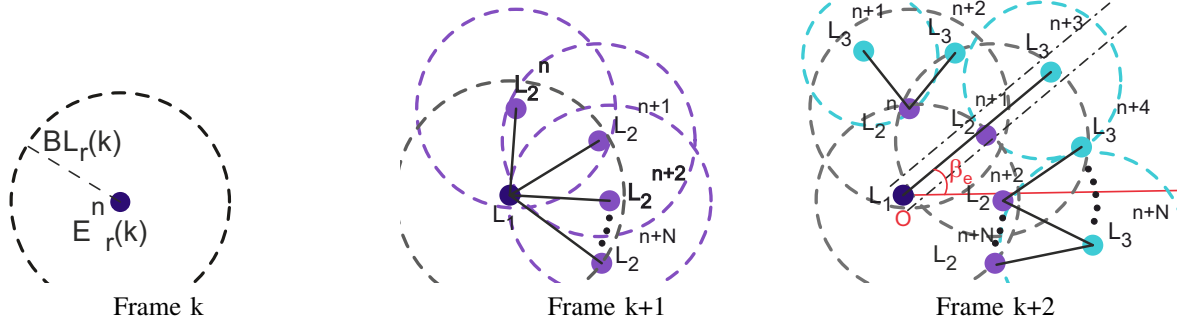


Fig. 4. Rebel landmarks orientation detection through the three key step frames. The dashed gray lines are the previous steps boundary layers, the dot-dashed lines are the error span variation's space. The remaining colorized dashed circles are corresponding standard BL size for obtained marks.

mulation. The initial values for E_r is constructed as following:

$$\begin{aligned}
 DL_{E_r0} &= \hat{L}_{3-1} - \hat{L}_{2-1} \\
 V_{E_r0} &= \frac{L_3 - L_2}{t_f} \\
 \beta_{E_r0} &= \hat{L}_{3-1} \\
 O_{E_r0} &= L_1
 \end{aligned} \quad (6)$$

Where, for a example, \hat{L}_{3-1} presents angle of a constructed line from point 3 with respect to 1. For existing rebel landmarks the parameters L , V_r are estimated as equations (4),(6) except DL is updated as:

$$DL_{E_r}(k) = DL_{E_r}(k-1) - [\beta_{E_r}(k) - \beta_{E_r}(k-1) - DL_{E_r}(k-1)] \quad (7)$$

Addition to these, the $\beta_{E_r}(k)$ is just calculated from last detected edge respect to rebel edges origin O . These possible outcomes help us for having the detection and learning to be smooth and we would have similar appliance of negative and positive classified examples [14]. In contrast, we use gradual machine-learning with disappearing pattern via truth definition. These assumptions with designed constraints and dynamic parameters can be seen as the main functioning point in the Circle expert. Algorithm 2 is showing the main execution codes in preparing the rebel and normal circles. This designed algorithm is divided to three main parts. First part detects and compares the *Edge* with E_n group. Next, after elimination, remaining unmatched landmarks are carried to second part for E_r rebel edges study. The latest E_n and E_r matrices are compared under giving constraints to develop the latest circles.

3) *Normal Edge Circling*: These landmarks are following the flow of vector field and group depending on their direction and velocities. To match these models, Fig. 5 is considered to form the circles.

Basically, kinematic estimation over the edges helps prepare the semi-autonomous system to evaluate its form with dependency on grouped edges in *Edge*. In this analysis, estimated circle from previous data and overwritten circle with obtained estimated edges are involved. This property is applied while it is within BS_λ region. For grouping E_n s depending on their

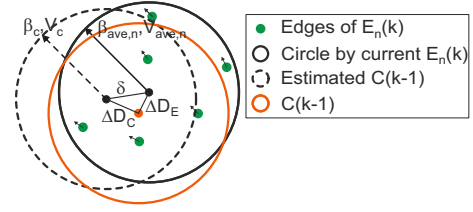


Fig. 5. Normal edges circle modeling.

angle and velocity for both initialization and circle comparison below formulas are applied.

$$\begin{cases} (\beta_{E_{nref.}} - \varepsilon_\beta) < \beta_{E_n}^i < (\beta_{E_{nref.}} + \varepsilon_\beta) \\ |V_{E_n}^i| \leq \varepsilon_V V_V \end{cases} \quad 1 < i \leq M \quad (8)$$

The ε depending on the required accuracy and distributional numbers can be carried to find proper constraints. Next, to compare the existing C_n , we have:

$$\begin{aligned}
 \left(\frac{\sum \beta_{E_n}}{M+1} - \varepsilon_\beta \right) < \beta_{C_n}^i < \left(\frac{\sum \beta_{E_n}}{M+1} + \varepsilon_\beta \right) \\
 \frac{|\sum V_{E_n}|}{M+1} \leq \varepsilon_V V_{C_n}^i
 \end{aligned} \quad (9)$$

Before applying these comparators, a weighting function takes place to evaluate the percentage of involvement about right circle in the these collected E_n .

$$\% \{ (L_{E_n}^i - L_{C_n}) < R_{C_n} \} < \% Cte \quad (10)$$

Back to the circle estimation, the ΔD_C and ΔD_E are calculated with simple trigonometric formulations, and proportional to the δ and trust value of circles, the reliable circle is optimized. As an important case, while circle's angle is aligned with average grouped E_n with defined ε_β , the corresponding circle is upgraded with +1 trust. However, if angle is deviated despite major inclusion of edges in the circle, it is updated with decreasing trust.

4) *Rebel Edge Circling*: Conspicuously, the most of objects won't have constant flow on the frame. These objects normally will be the ones that have potential to come toward or critically approach the captured camera. Therefore, rebellious detected

Algorithm 3 Circle Expert, Circle Estimation Part

```

1: procedure CIRCLE( $Edge, C_n, C_r, E_n, E_r, \psi, \delta, V_v, D_v$ )
2:   if  $C_n = \emptyset \ \& \ E_n \neq \emptyset$  then            $\triangleright C_n$  matching
3:     Initialize  $C_n$ 
4:   else
5:     while All the circles in  $C_n$  are checked do
6:       while All the edges in  $E_n$  are checked do
7:         Group  $E_n$ 
8:         if Grouped  $E_n$  satisfies normal edge aligned
9:            $N^{th} C'_n$  then
10:            Update  $N^{th} C_n$ 
11:          else if Grouped  $E_n$  satisfies normal edge
12:            deviated  $N^{th} C'_n$  then
13:              Update  $N^{th} C_n$ 
14:            end if
15:          end while
16:        end while
17:        Update not matched  $C_n$  with  $C'_n$ 
18:        Create new  $C_n$  from left  $E_n$ 
19:      end if            $\triangleright C_n$  matching
20:    if  $C_r = \emptyset \ \& \ E_r \neq \emptyset$  then        $\triangleright C_r$  matching
21:      Initialize  $C_r$ 
22:    else
23:      while All the rebel circles in  $C_r$  are checked do
24:        while All the edges in  $E_r$  are checked do
25:          Group  $E_r$ 
26:          if Grouped  $E_r$  satisfies rebel circle aligned
27:             $N^{th} C'_r$  then
28:              Update  $N^{th} C_r$ 
29:            else if Grouped  $E_r$  satisfies rebel circle
30:              deviated  $N^{th} C'_r$  then
31:                Update  $N^{th} C_r$ 
32:              end if
33:            end while
34:          end while
35:          Update not matched  $C_r$  with  $C'_r$ 
36:          Create new  $C_r$  from left  $E_r$ 
37:        end if            $\triangleright C_r$  matching
38:      if Any  $C_n$ 's  $Tr$  satisfies  $Tr_{max}$  then
39:        Update  $\psi$ 
40:        Refresh  $Tr$ 
41:      end if
42:    Update  $\lambda$  by  $C_n$  and  $C_r$ 
43:  return  $C_n, C_r, \lambda, \psi$ 
44: end procedure

```

edges will have most importance when it comes to SLAM or object avoidance applications. The rebel landmarks in the worst case scenario can be appeared within the normal edge circles [see Fig. 6]. To evaluate these formats, the previous available similar edges are considered with specific dedication to the β_{C_r} and V_{C_r} . Furthermore, it must be considered these edges are the hardest ones since they are not following vectors field flow when they are having a displacement on frame. Thus,

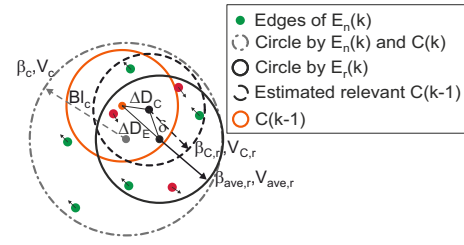


Fig. 6. Rebel edges circle modeling, Note: Red dots are detected rebel edges.

it is not able to carry out with accurate reliance on the next frame similar velocity edges in surrounding area of located ones. Therefore, the equation (8) is improved as:

$$\begin{cases} (\beta_{E_{ref.}} - \varepsilon_\beta) < \beta_{E_r}^i < (\beta_{E_{ref.}} + \varepsilon_\beta) & 1 < i \leq M \\ |V_{E_{ref.}}| \leq (V_{E_r}^i + \varepsilon_v V_v) \end{cases} \quad (11)$$

Velocity constraint is largely dependent on rebel edges estimated velocities. Before estimation, we have to track the circle in which is using the same technique (10). Next, the comparator is evaluating the grouped rebel edges with each C_r as following:

$$\begin{aligned} & \left(\frac{\sum [\beta_{E_r} + DL_{E_r}]}{M+1} - \varepsilon_\beta \right) < \beta_{C_r}^i < \left(\frac{\sum [\beta_{E_r} + DL_{E_r}]}{M+1} + \varepsilon_\beta \right) \\ & \frac{|\sum V_{E_r}|}{M+1} \leq (V_{C_r}^i + \varepsilon_v V_v) \end{aligned} \quad (12)$$

Lastly, the same evaluation for locating rebel circles are taken place as C_n . In general, other parameters (i.e. L_{C_r} , R_{C_r} and Tr) updates look like the normal circle process except in the estimation, β_{C_r} is updating every time with inclusion of $\frac{\sum [\beta_{E_r} + DL_{E_r}]}{M+1}$.

III. RESULTS AND DISCUSSION

In our experiment, we use IMU Samsung sensor integrated with XP HD camera to apply our filter with images resolution of 640×480 pixels. The study takes place with the worst case scenario where the frame rate is at 1 frame/sec. Although, the geometric filter shows its best performance in at least 3 frame/sec, due to low velocity in vehicle ($V_v = 5 \text{ Cm/s}$) and minor acceleration 0.1 Cm/s^2 , robot can perfectly perform in detecting required edges and passing/incoming objects. In the edge detection technique FAST9 with 25 point threshold is utilized [3], [12]. The environment is chosen with overwhelming landmark properties over 1000 edges spaces. To perfectly apply the algorithm on our trust parameters are determined as $Tr_s = 3$, $Tr_{cr} = 2$ and $Tr_{max} = 5$. Additionally, the angular error related to δ_{y-z}^v is 4 pixel on average. The center of the image is in the coordinate location of 320×240 . Boundary layer (BL) for initialization of normal edges and detection constant property for rebel edges is 25 pixels. The circling approximated ε coefficients are $\varepsilon_\beta = 20^\circ$ and $\varepsilon_v = 10$ for equation (8) and also $\varepsilon_\beta/5$ and $10 \varepsilon_v$ for (9). For rebel circle

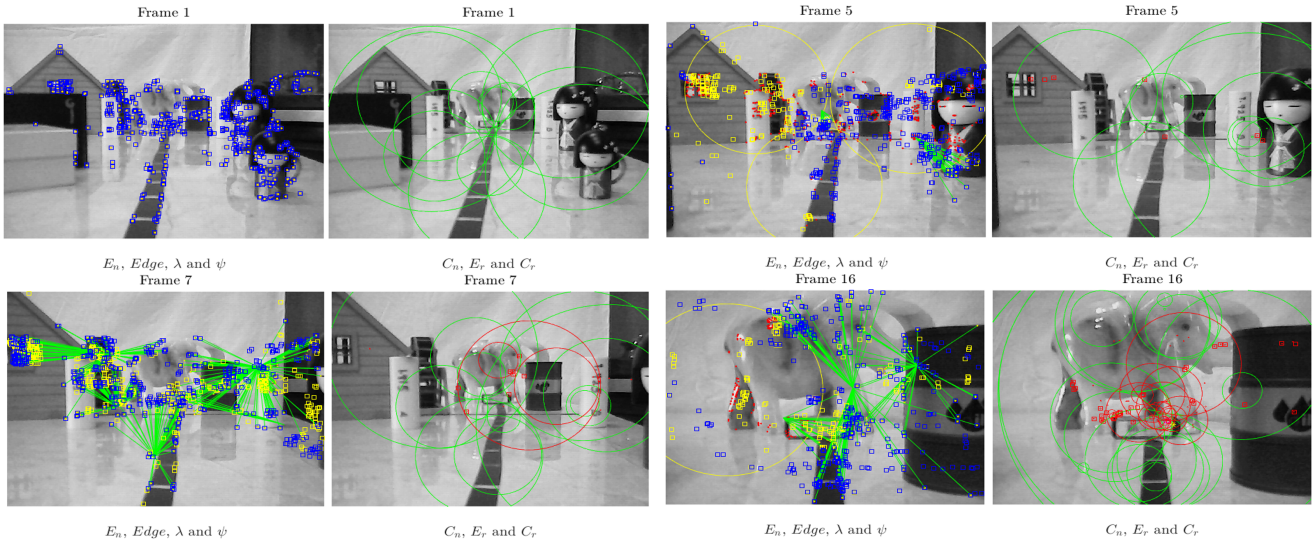


Fig. 7. Captured frames of experiment in real-time with camera.

coefficients about equation (11), ε_β and ε_v are 50° and 40 . Additionally, $\varepsilon_\beta = 10^\circ$ and $\varepsilon_v = 1000$ are for last equation (12). Percentage of involvement for both circling algorithms are 50%. The rest of governing parameters in algorithms, are using empty matrices as initial conditions.

The results are demonstrated with four sampled images as Fig. 7. The total demonstration has been made available online.¹ The presentation has two main alike images. The left side image shows the detected edges with yellow color by FAST9 corner detection algorithm. However, red color points are the omitted ones that detected but is ignored by our filter. Also, the filter latest estimations with our algorithm are shown with blue squares. To present the pure estimation by dynamic equations of motion related to objects, the yellow square graphs are involved. Lastly, to present λ and ψ , specifically centered connected green lines and yellow circles are used. On the right hand side image, the C_n and C_r are using green and red circles respectively. Lastly, The square graphs are presenting our filters latest E_r estimations in the motion of camera.

As a highlighted captured frames, in first frame, the filter tries to initialize the scene by recording all detected edges to E_n and preparing normal circles relative to velocity and angle constraints of C_n . To compare and sense the change in our experts Frame 5 and 7 are chosen. After, obtaining required trust about certain landmarks with true detection, the ψ is activated to decrease the unwanted calculations. Also, in frame 5, the detected rebel edges results a approximated incoming objects orientations to inform the user. In next frame, it becomes obvious that beside reactivating ignored areas with having automatic edge approximations for those regions, Circle expert tries to locate the previous frames circles which are relative to the objects locations. It is clear that filter let us with minimum frame/rate to detect majority of incoming whole objects or their particular regions. Finally, to

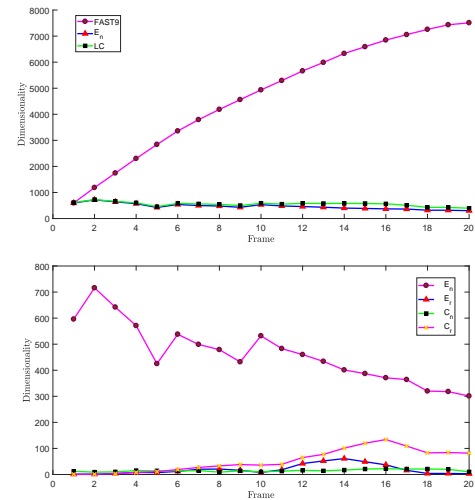


Fig. 8. Dimensionality of the LC filter and FAST9 SLAM. Note: the last figure shows LC's each parameter occupying space.

one of the last frames (frame 16) with clear incoming objects toward camera, the rebel edge detection with its pure dynamic estimation (purple square), detected current rebel edge (star point) and latest filter estimation (red square) are illustrated. The success of filter can be clearly seen that majority of rebel edges were estimated by filter truly without having clear incoming current frame data. Lastly, the Fig. 8 shows that how far the LC filter have computation space in contrast to the FAST9 SLAM. As it is clear, the LC filter dimensionality follows decreasing rate with latest sampled frame at 300. As an interesting fact, although complexity of images with inclusion edges increases, normal circles tries to eliminate overwhelming created edges from normal passing landmarks.

¹Online available experimental result.

IV. CONCLUSION

In this paper, we present the integrated geometric LC filter that consists of two experts. The first expert is dealing with collecting the data relative to feedback of circle expert. Detection, learning and tracking all take place inside Circle expert. As an interesting result, beside considerable decrease in matrix sizes in the computations, the model operates smooth follow that let the model act spontaneously with having efficient forgetting and ignoring abilities during continues operations. The ignorance also permit us to avoid any problem during entrance to immense landmark area.

We are planning to apply error estimation matrix to both experts for operating the filter faster and more accurate in our incoming works. We hope it will be a high potential candidate instead of Kalman Filter. This will help us automate the trust factor perfectly within dynamic scenes. Also, it will be applied on agile non-holonomic robots with rotational plain motions [15], [16] to perfectly evaluate the scene properties. Lastly, the filter will be improved as Line-Circle-Square model to completely detect each corresponding objects in the scene.

REFERENCES

- [1] H. Lategahn and C. Stiller, "Vision-only localization," *IEEE Transactions on Intelligent Transportation Systems*, vol. 15, no. 3, pp. 1246–1257, June 2014.
- [2] J. Xiao, T. Fang, P. Tan, P. Zhao, E. Ofek, and L. Quan, "Image-based façade modeling," *ACM Trans. Graph.*, vol. 27, no. 5, pp. 161:1–161:10, Dec. 2008.
- [3] E. Rosten and T. Drummond, "Machine learning for high-speed corner detection," in *European Conference on Computer Vision*, Berlin, Heidelberg, 2006, pp. 430–443.
- [4] D. Murray and J. J. Little, "Using real-time stereo vision for mobile robot navigation," *Autonomous Robots*, vol. 8, no. 2, pp. 161–171, 2000.
- [5] P. Sand and S. Teller, "Particle video: Long-range motion estimation using point trajectories," *International Journal of Computer Vision*, vol. 80, no. 1, p. 72, 2008.
- [6] C. Bibby and I. Reid, "Robust real-time visual tracking using pixel-wise posteriors," in *Proceedings of European Conference on Computer Vision*, 2008.
- [7] S. Pillai and J. Leonard, "Monocular slam supported object recognition," in *Proceedings of Robotics: Science and Systems*, Rome, Italy, July 2015.
- [8] Z. Sun, G. Bebis, and R. Miller, "On-road vehicle detection: a review," *IEEE Transactions on Pattern Analysis and Machine Intelligence*, vol. 28, no. 5, pp. 694–711, May 2006.
- [9] V. Lui and T. Drummond, "Image based optimisation without global consistency for constant time monocular visual slam," in *2015 IEEE International Conference on Robotics and Automation (ICRA)*, May 2015, pp. 5799–5806.
- [10] D. Gamage and T. Drummond, "Reduced dimensionality extended kalman filter for slam in a relative formulation," in *2015 IEEE/RSJ International Conference on Intelligent Robots and Systems (IROS)*, Sept 2015, pp. 1365–1372.
- [11] P. Lichtsteiner, C. Posch, and T. Delbruck, "A 128x128 120 dB 15 μ s latency asynchronous temporal contrast vision sensor," *IEEE Journal of Solid-State Circuits*, vol. 43, no. 2, pp. 566–576, Feb 2008.
- [12] E. Rosten, R. Porter, and T. Drummond, "Faster and better: A machine learning approach to corner detection," *IEEE Transactions on Pattern Analysis and Machine Intelligence*, vol. 32, no. 1, pp. 105–119, Jan 2010.
- [13] J. Y. Bouguet, "Pyramidal implementation of the lucas kanade feature tracker," *Technical report, Microprocessor Research Labs*, 2000.
- [14] Z. Kalal, K. Mikolajczyk, and J. Matas, "Tracking-learning-detection," *IEEE Transactions on Pattern Analysis and Machine Intelligence*, vol. 34, no. 7, pp. 1409–1422, July 2012.
- [15] S. A. Tafrishi, S. M. Veres, E. Esmaeilzadeh, and M. Svinin, "Dynamical behavior investigation and analysis of novel mechanism for simulated spherical robot named "RollRoller"," *ArXiv*, 2016, Available at <http://arxiv.org/abs/1610.06218>.
- [16] S. A. Tafrishi, M. Svinin, and E. Esmaeilzadeh, "Effects of the slope on the motion of spherical rollroller robot," in *2016 IEEE/SICE International Symposium on System Integration (SII)*, Dec 2016, pp. 875–880.